

Boundary Induced Vibration and Dynamic Stiffness of a Sagging Cable

Uwe Starossek

Institut für Tragwerksentwurf und -konstruktion
Universität Stuttgart

ABSTRACT: This paper sets forth the linear theory of boundary induced vibration of an extensible, sagging cable. A dynamic stiffness matrix is derived whose coefficients are functions of the frequency of motion, and which is suitable for dynamic direct-stiffness analysis of complex systems. The study considers motion within the cable plane only. Viscous damping is taken into account.

1 Introduction

The static analysis of a mechanical system usually requires knowledge of the load-deformation behavior of the system elements. This behavior can be described in compact form by stiffness matrices. Limited to the steady-state response, it is possible to transfer this concept to the investigation of dynamic processes, which implies the development of dynamic impedance or stiffness matrices [1].

In this paper, the dynamic stiffness matrix of an extensible, flexible and sagging cable is derived. This matrix can be utilized for the dynamic analysis of composed systems such as cable-stayed bridges or guyed masts. The cable is considered as a continuum. Only small displacements are admitted (linear theory) and only motions and forces within the vertical cable plane are regarded. Viscous damping — for example, due to external fluid forces — is taken into consideration.

As far as it is known, previous solutions to the defined problem have been confined essentially to one element of the here computed 4*4 matrix: the horizontal stiffness at the upper end of an inclined cable which is fixed at the lower end.

Treatises by Davenport & Steels [7] and Irvine [3] give formulas which according to the findings of this study are not sufficiently precise for tightly stretched inclined cables. Paper [7] also considers damping, but the numeric evaluation of infinite series is required. Veletsos & Darbre [8] have developed a more accurate closed-form expression for the damped cable which can be transformed into the corresponding element of the matrix derived here, although a small correction must be made.

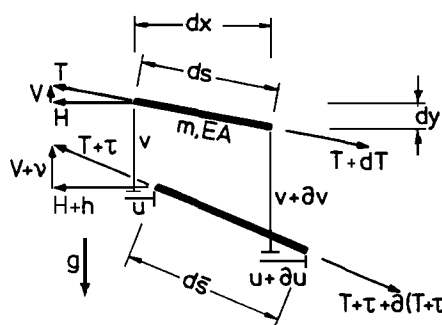
This study partly follows the course revealed by Irvine & Caughey [2] and Irvine [3] and [4], but the scope is different (stiffness matrix) and greater generality is obtained (damping). Initially, the derivation proceeds in a local coordinate system and is valid for a horizontal cable. The result is then generalized to apply to an inclined cable and transformed to global coordinates. In addition to the derivation of the stiffness matrix, the dynamic cable displacement is evaluated as a function of the boundary displacements. A discussion of example calculations, as well as a detailed comparison to the results of other authors, conclude this paper.

The conditions and limits of validity of the theory are worked out here in more detail than in previous publications. Comprehensive derivation of basic equations and exhaustive review of intermediate stages were therefore necessary.

The utilization of trigonometrical solution functions with complex arguments is novel and remarkable; with the help of these functions, the analysis of damped cable vibrations can be managed with astonishing elegance. Beyond the particular problem discussed herein, this method may be applied to most kinds of damped oscillations which can be described by linear differential equations.

2 Basic Equations

The equations of static equilibrium of a differential cable segment are (see figure 1)



$$\frac{d}{ds} \left(T \frac{dy}{ds} \right) = -mg \quad (1)$$

$$\frac{d}{ds} H = 0 \quad , \quad (2)$$

Figure 1. Differential cable element

in which T represents the static cable tension, and

$$H = T \frac{dx}{ds} \quad (3)$$

its horizontal component; m is the cable mass per unit length and g is the gravitational acceleration (in reference to m and g , see the closing remarks of section 5). The static form of a horizontal cable is approximated by a quadratic parabola. It follows, using the terms of figure 2, that

$$y = \frac{mg l^2}{2H} \left[\frac{x}{l} - \left(\frac{x}{l} \right)^2 \right] \quad (4)$$

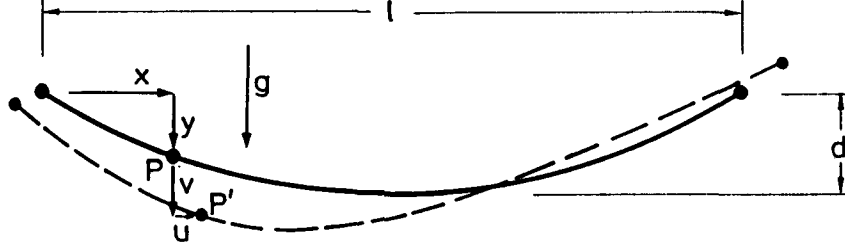


Figure 2. Horizontal cable

The relation between the quantities already introduced and the static sag at midspan $d = y|_{x=l/2}$ then is

$$H = \frac{mg l^2}{8d} . \quad (5)$$

The equations previously presented by Irvine & Caughey [2] for the description of dynamic equilibrium and continuity of the cable element are derived here in detail in order to precisely develop the preconditions and valid definitions.

In order to drastically simplify the problem, a statement first is made regarding the dynamic part τ of the total cable tension. The velocity of the elastic wave in a rod is

$$c_e = \sqrt{\frac{EA}{m}} , \quad (6)$$

where EA is elastic resistance. It is valid for the velocity of transverse waves in a horizontal cable (when the sag is shallow) that

$$c_v = \sqrt{\frac{H}{m}} . \quad (7)$$

For a steel cable with a modulus of elasticity of $E = 200\,000$ MPa and a cable stress of $\sigma \leq 500$ MPa, the ratio of the two wave speeds becomes

$$\frac{c_e}{c_v} = \sqrt{\frac{EA}{H}} \simeq \sqrt{\frac{E}{\sigma}} \geq 20 \gg 1 . \quad (8)$$

Because of the wide numerical distance between the velocities, it is possible to identify two kinds of vibration modes, which are associated with either predominantly geometrical or predominantly elastic deformation. The ratio of the pertinent frequencies corresponds approximately to the speed ratio of eq. (8).

If the study is restricted to frequencies within the range of the first (geometrical) natural frequencies, the elastic deformation may be supposed to be quasi-static; the

inertial forces in cable direction will be too small to effect a significant variation of the dynamic cable tension τ along the cable. Thus the approximation

$$\frac{\partial \tau}{\partial x} = 0 \quad (9)$$

is valid. This equation replaces the equation of dynamic equilibrium in the horizontal direction.

The dynamic equilibrium of the vertical forces is guaranteed if

$$\frac{\partial}{\partial s} [(T + \tau) \varphi_y] = m \frac{\partial^2 v}{\partial t^2} - mg \quad , \quad (10)$$

where the vertical component of the total cable tension is obtained through multiplication by

$$\varphi_y := \frac{dy + \partial v}{d\bar{s}} \quad (11)$$

(see figure 1). The damping influence is neglected for the present.

After introduction of the elastic strain

$$\varepsilon := \frac{\partial \bar{s}}{\partial s} - 1 \quad (12)$$

it is valid from linearized analysis that

$$\begin{aligned} \varphi_y &= \frac{dy + \partial v}{ds} \frac{1}{1 + \varepsilon} \\ &= \frac{dy + \partial v}{ds} (1 - \varepsilon + \varepsilon^2 - \dots) \\ &= \left(\frac{dy}{ds} + \frac{\partial v}{\partial s} \right) (1 - \varepsilon) \quad . \end{aligned} \quad (13)$$

Subsequent insertion in eq. (10), taking into consideration eq. (1) and referring to the fundamental equation of elasticity

$$EA \cdot \varepsilon = \tau \quad (14)$$

leads to the linearized equation

$$\frac{\partial}{\partial s} \left[T \frac{\partial v}{\partial s} + \tau \frac{dy}{ds} \left(1 - \frac{T}{EA} \right) \right] = m \frac{\partial^2 v}{\partial t^2} \quad , \quad (15)$$

which, with the application of expressions (2), (3) and (9), is simplified to

$$H \frac{\partial^2 v}{\partial x^2} + \tau \frac{d}{dx} \left(\frac{dy}{ds} - \frac{H}{EA} \frac{dy}{dx} \right) = m \frac{ds}{dx} \frac{\partial^2 v}{\partial t^2} \quad . \quad (16)$$

The interposed derivations

$$\frac{d}{dx} \frac{dy}{ds} = \frac{d}{dx} \left(\frac{dy}{dx} \frac{dx}{ds} \right) = \frac{d^2y}{dx^2} \frac{dx}{ds} + \frac{dy}{dx} \frac{d}{dx} \left(\frac{dx}{ds} \right)^{-1}$$

and

$$\frac{d}{dx} \left(\frac{dx}{ds} \right)^{-1} = \frac{d}{dx} \left[1 + \left(\frac{dy}{dx} \right)^2 \right]^{-\frac{1}{2}} = - \left(\frac{dx}{ds} \right)^3 \frac{dy}{dx} \frac{d^2y}{dx^2} \quad (17)$$

and from this

$$\frac{d}{dx} \frac{dy}{ds} = \frac{dx}{ds} \frac{d^2y}{dx^2} \left[1 - \left(\frac{dy}{ds} \right)^2 \right] = \left(\frac{dx}{ds} \right)^3 \frac{d^2y}{dx^2} \quad (18)$$

are made. Hence eq. (16) leads to

$$H \frac{\partial^2 v}{\partial x^2} + h_\tau \frac{d^2 y}{dx^2} \left[\left(\frac{dx}{ds} \right)^2 - \frac{H}{EA} \frac{ds}{dx} \right] = m \frac{ds}{dx} \frac{\partial^2 v}{\partial t^2} \quad (19)$$

The quantity h_τ is defined, equivalently to eq. (3), as

$$h_\tau := \tau \frac{dx}{ds} \quad (20)$$

With a sufficiently small sag ($d/l \leq 1/20$), the differentials dx/ds and ds/dx in eq. (19) can be replaced by unity. Moreover, when the part related to H/EA is omitted — this value was already assumed to be small in the derivation — an equation of motion which formally coincides with the expression given by Irvine & Caughey [2] is obtained.

It is thus possible to derive this relation without a limitation of the horizontal displacement u ! It can therefore be taken as a basis for the analysis of a cable with displaceable boundaries which is presented herein.

Considering, in addition, a viscous damping force which acts on the swinging cable from an ambient medium, the equation of motion valid for sufficiently taut cables

$$H \frac{\partial^2 v}{\partial x^2} + h_\tau \frac{d^2 y}{dx^2} = m \frac{\partial^2 v}{\partial t^2} + c \frac{\partial v}{\partial t} \quad (21)$$

is obtained. Here c is the damping force per unit length and velocity. In the case of horizontally displaceable boundaries, the damping force in the vicinity of the boundaries is predominantly determined by $\partial u / \partial t$ rather than by $\partial v / \partial t$. The corresponding effect on the global behavior, however, is comparatively little (if a shallow sag is assumed) and is neglected.

The derivation of the second basic equation proceeds from eq. (14). Equation (12) and

$$d\bar{s} = \left[(dx + \partial u)^2 + (dy + \partial v)^2 \right]^{\frac{1}{2}} \quad (22)$$

lead to

$$\varepsilon = \frac{dx}{ds} \frac{\partial u}{\partial s} + \frac{dy}{ds} \frac{\partial v}{\partial s} \quad (23)$$

for the cable strain ε when terms of the second order are neglected. Through the substitution of eq. (23) into eq. (14) and the application of definition (20), the equation

$$\frac{h_\tau}{EA} \left(\frac{ds}{dx} \right)^3 = \frac{dy}{dx} \frac{\partial v}{\partial x} + \frac{\partial u}{\partial x} \quad (24)$$

is obtained, which again formally conforms to the equation presented by Irvine & Caughey [2]. It provides for the elastic and geometric compatibility of the cable element.

Instead of the dynamic part h of the total horizontal force, the auxiliary quantity h_τ as defined in eq. (20) appears here. A distinction between these values is made, as h according to fig. 1 is

$$h = (T + \tau) \varphi_x - T \frac{dx}{ds} , \quad (25)$$

which, when the term

$$\begin{aligned} \varphi_x &:= \frac{dx + \partial u}{d\bar{s}} \\ &= \frac{dx + \partial u}{ds} \frac{1}{1 + \varepsilon} = \left(\frac{dx}{ds} + \frac{\partial u}{\partial s} \right) (1 - \varepsilon) \end{aligned} \quad (26)$$

is substituted (cf. eq. (13)), becomes

$$h = h_\tau \left(1 - \frac{H}{EA} \frac{ds}{dx} \right) + H \frac{\partial u}{\partial x} . \quad (27)$$

When utilizing eq. (24), $\partial u / \partial x$ can be eliminated. The term which then is related to H/EA is again neglected and the equation

$$h = h_\tau - H \frac{dy}{dx} \frac{\partial v}{\partial x} \quad (28)$$

is obtained, from which the dynamic horizontal force can be determined as a function of h_τ and $\partial v / \partial x$.

The dynamic part ν of the total vertical force may be written

$$\nu = (T + \tau) \varphi_y - T \frac{dy}{ds} . \quad (29)$$

From eqs. (13) and (14), it follows that

$$\nu = h_\tau \frac{dy}{dx} \left(1 - \frac{H}{EA} \frac{ds}{dx} \right) + H \frac{\partial v}{\partial x} . \quad (30)$$

Neglecting the term related to H/EA

$$\nu = h_\tau \frac{dy}{dx} + H \frac{\partial v}{\partial x} \quad (31)$$

ultimately is obtained.

3 Dynamic Behavior of the Horizontal Cable

3.1 General Terms

A cable with moderate sag ($d/l \leq 1/20$) is investigated. Its ends are supported at the same level. It is assumed that the vibration is described by the products

$$v(x, t) = \tilde{v}(x) e^{i\omega t} \quad (32a)$$

$$u(x, t) = \tilde{u}(x) e^{i\omega t} , \quad (32b)$$

where

$$\tilde{u}, \tilde{v}, \omega \in \mathcal{C} ; \quad i^2 = -1 .$$

Consequently, the expressions

$$h_\tau(x, t) = \tilde{h}_\tau(x) e^{i\omega t} ; \quad \tilde{h}_\tau \in \mathcal{C} \quad (32c)$$

$$\tau(t) = \tilde{\tau} e^{i\omega t} ; \quad \tilde{\tau} \in \mathcal{C} \quad (32d)$$

will hold and analogous product descriptions are valid for the boundary forces and displacements. That is, only harmonic vibrations and vibrations with an exponentially variable amplitude (modified-harmonic vibrations) are admitted. With

this approach, the steady-state system response to harmonic excitation, as well as damped free vibrations, can be investigated.

In every case, the dynamic stiffness functions are defined as time-independent relations between boundary forces and boundary displacements of the cable as a part of a vibrating system.

With the adoption of approach (32) and the use of the static relations (4) and (5), the equation of motion (21) leads to the ordinary differential equation

$$H \frac{\partial^2 \tilde{v}}{\partial x^2} + \omega_c^2 m \tilde{v} = \frac{8d}{l^2} \tilde{h}_\tau, \quad (33)$$

which here is considered inhomogeneous. The introduction of the auxiliary parameter

$$\omega_c := \omega \sqrt{1 - 2\xi i}, \quad \text{where} \quad \xi := \frac{c}{2m\omega}, \quad (34)$$

provides a substantial simplification of further derivations. They can now be formally carried out as if damping were not present! The definition of the dimensionless quantities

$$\Omega := \omega l \sqrt{\frac{m}{H}}, \quad \Omega_c := \omega_c l \sqrt{\frac{m}{H}} \quad (35)$$

will later prove useful.

From the compatibility condition (24),

$$\frac{\tilde{h}_\tau}{EA} \left(\frac{ds}{dx} \right)^3 = \frac{dy}{dx} \frac{\partial \tilde{v}}{\partial x} + \frac{\partial \tilde{u}}{\partial x} \quad (36)$$

is obtained.

This investigation now proceeds separately for horizontal and vertical boundary displacements. A distinction between symmetric and antisymmetric contributions is made.

In view of the presumed small sag, the quantity h_τ is now regarded — similarly to τ — as spatially constant, especially in respect to the integrations subsequently performed.

3.2 Horizontal Boundary Displacements

Symmetric:

The dynamic stiffness functions defined as



$$k_{h,u}^s := \frac{h^s}{u^s} = \frac{\tilde{h}^s}{\tilde{u}^s} \quad (37a)$$

$$k_{\nu,u}^s := \frac{\nu^s}{u^s} = \frac{\tilde{\nu}^s}{\tilde{u}^s} \quad (37b)$$

Figure 3. Horizontal boundary displacement (symmetric)

are computed (see the notations of figure 3). The solution of eq. (33), adapted to the valid boundary conditions, is

$$\tilde{v} = \frac{8d}{\Omega_c^2 H} \tilde{h}_\tau \left(1 - \tan \frac{\Omega_c}{2} \sin \frac{\Omega_c x}{l} - \cos \frac{\Omega_c x}{l} \right) , \quad (38)$$

which is easily shown by substitution. The arguments of the trigonometrical solution functions are complex. The integration of eq. (36) makes it possible to eliminate the displacement function $\tilde{u}(x)$. By utilizing eqs. (4) and (5),

$$\frac{\tilde{h}_\tau L_e}{EA} = \tilde{u}^s + \frac{8d}{l^2} \int_0^l \tilde{v} dx \quad (39)$$

is obtained, where

$$L_e := \int_0^l \left(\frac{ds}{dx} \right)^3 dx \simeq l \left[1 + 8 \left(\frac{d}{l} \right)^2 \right] . \quad (40)$$

Substituting the expression (38) into the integral formula (39) and solving for \tilde{h}_τ yields

$$\tilde{h}_\tau = \frac{EA}{L_e} \frac{1}{1 + \frac{\lambda^2}{\Omega_c^2} (\kappa - 1)} \tilde{u}^s , \quad (41)$$

where

$$\lambda^2 := \left(\frac{mgl}{H} \right)^2 \frac{EA l}{HL_e} \quad (42)$$

is the fundamental cable parameter and

$$\kappa = \kappa(\Omega_c) := \frac{\tan(\Omega_c/2)}{\Omega_c/2} \quad (43)$$

is an auxiliary function dependent solely on Ω_c .

The dynamic horizontal force at the boundary \tilde{h}^s is obtained from eq. (28), where now the terms

$$\left. \frac{dy}{dx} \right|_{x=0} = \frac{1}{2} \epsilon \quad (44)$$

$$H \left. \frac{\partial \tilde{v}}{\partial x} \right|_{x=0} = -\frac{1}{2} \epsilon \kappa \tilde{h}_\tau \quad (45)$$

are substituted. The expression

$$\tilde{h}^s = \left(1 + \frac{1}{4} \epsilon^2 \kappa \right) \tilde{h}_\tau, \quad (46)$$

is obtained, where the quantity

$$\epsilon := \frac{mgl}{H} = \frac{8d}{l} \quad (47)$$

as here defined approximately corresponds to the ratio of the total cable weight to the average static cable tension. After substitution of eq. (41) into eq. (46), the first stiffness function

$$k_{\tilde{h},u}^s = \frac{EA}{L_e} \frac{1 + \frac{1}{4} \epsilon^2 \kappa}{1 + \frac{\lambda^2}{\Omega_c^2} (\kappa - 1)} \quad (48)$$

as defined by eq. (37a) is obtained. For strongly tightened steel cables with $\epsilon \ll 1$, the second term in the numerator can be of significance only in the nearest vicinity of singularities, that is, for example, for

$$\Omega_c \simeq (2n - 1)\pi; \quad n = 1, 2, \dots$$

By neglecting it, the simplified expression

$$k_{h,u}^s = \frac{EA}{L_e} \frac{1}{1 + \frac{\lambda^2}{\Omega_c^2} (\kappa - 1)} \quad (49)$$

is obtained. Upon carrying out the limiting transition $\Omega_c \rightarrow 0$, eq. (48) becomes

$$k_{h,u}^s \Big|_{\Omega_c \rightarrow 0} = \frac{EA}{L_e} \frac{1 + \frac{1}{4}\epsilon^2}{1 + \frac{1}{12}\lambda^2} \simeq \frac{EA}{l} \frac{1}{1 + \frac{1}{12}\lambda^2} , \quad (50)$$

which coincides — as expected — with the well-known formula for static equivalent stiffness.

From equation (31), the dynamic vertical force results in

$$\tilde{\nu}^s = -\tilde{\nu} \Big|_{x=0} = \frac{1}{2}\epsilon(\kappa - 1) \tilde{h}_\tau , \quad (51)$$

whereupon the second stiffness function, defined by eq. (37b), becomes

$$k_{\nu,u}^s = \frac{EA}{L_e} \frac{\frac{1}{2}\epsilon(\kappa - 1)}{1 + \frac{\lambda^2}{\Omega_c^2} (\kappa - 1)} . \quad (52)$$

It is easily verified that this function — as it must — vanishes for $\Omega_c \rightarrow 0$ and is positive for small real Ω_c .

The vertical displacement \tilde{v} , which corresponds to the boundary displacement \tilde{u}^s , can be calculated by making use of eqs. (38) and (41). The result is

$$\left. \begin{aligned} \tilde{v} &= \beta_u^s \cdot \tilde{u}^s \\ \beta_u^s &:= \frac{1}{\epsilon \Omega_c^2} \frac{\lambda^2}{1 + \frac{\lambda^2}{\Omega_c^2} (\kappa - 1)} \left[1 - \tan \frac{\Omega_c x}{l} \sin \frac{\Omega_c x}{l} - \cos \frac{\Omega_c x}{l} \right] . \end{aligned} \right\} \quad (53)$$

For the static case this reduces to

$$\tilde{v} \Big|_{\Omega_c \rightarrow 0} = -\frac{\lambda^2}{\epsilon} \frac{\frac{1}{2} \left[\frac{x}{l} - \left(\frac{x}{l} \right)^2 \right]}{1 + \frac{1}{12}\lambda^2} \tilde{u}^s . \quad (54)$$

Antisymmetric:

Here, the dynamic stiffness functions



$$k_{h,u}^a := \frac{h^a}{u^a} = \frac{\tilde{h}^a}{\tilde{u}^a} \quad (55a)$$

$$k_{\nu,u}^a := \frac{\nu^a}{u^a} = \frac{\tilde{\nu}^a}{\tilde{u}^a}, \quad (55b)$$

Figure 4. Horizontal boundary displacement (antisymmetric)

defined with reference to figure 4, are evaluated. Presupposing the existence of an antisymmetric solution for $\tilde{v}(x)$, the integration of eq. (36), when the governing boundary conditions are taken into account, results in a vanishing \tilde{h}_r . Equation (33), being homogeneous, in fact has antisymmetric solutions, in which ω_c , however, is no longer freely optional (because of likewise homogeneous boundary conditions); only the eigensolutions for a cable fixed at both ends can be found. A relation between the imposed boundary displacement u^a and the quantities v, h^a, ν^a can no longer be established! In order to do so, it would be necessary to consider the horizontal equilibrium condition which heretofore has been ignored, and so take into account the horizontal forces of inertia. Consistent development of the theory is provided by using the remaining trivial solution

$$\tilde{v} \equiv 0 \iff \beta_u^a := \frac{\tilde{v}}{\tilde{u}^a} \equiv 0. \quad (56)$$

Hence with eqs. (28) and (31) the stiffness functions become

$$k_{h,u}^a = 0 \quad (57)$$

$$k_{\nu,u}^a = 0. \quad (58)$$

For a rough estimate of the actual value of $k_{h,u}^a$, only the horizontal forces of inertia caused by an assumed rigid-body displacement are taken as a basis; from this

$$k_{h,u}^a = -\frac{1}{4}ml\omega_c^2 = -\frac{EA}{L_e} \frac{1}{4} \frac{\epsilon^2}{\lambda^2} \Omega_c^2 \quad (59)$$

is obtained. In comparison to eq. (49), this is actually of little influence and will be neglected. Under the previously specified restrictions (small sag and low frequency), the results according to eqs. (56), (57) and (58) will be utilized later in this paper. For the static case these equations become exact. As a result of the antisymmetric

deformation premise, and independent of the above discussion,

$$\tilde{v}_m = 0 \quad (60)$$

is found for the vertical displacement at midspan.

3.3 Vertical Boundary Displacements

Symmetric:

The dynamic stiffness functions defined as



$$k_{h,v}^s := \frac{h^s}{v^s} = \frac{\tilde{h}^s}{\tilde{v}^s} \quad (61a)$$

$$k_{\nu,v}^s := \frac{\nu^s}{v^s} = \frac{\tilde{\nu}^s}{\tilde{v}^s} \quad (61b)$$

Figure 5. Vertical boundary displacement (symmetric)

are calculated. For the boundary conditions defined in figure 5 the solution of eq. (33) is

$$\begin{aligned} \tilde{v} = & \frac{8d}{\Omega_c^2 H} \tilde{h}_\tau \left(1 - \tan \frac{\Omega_c}{2} \sin \frac{\Omega_c x}{l} - \cos \frac{\Omega_c x}{l} \right) \\ & + \frac{1}{2} \tilde{v}^s \left(\tan \frac{\Omega_c}{2} \sin \frac{\Omega_c x}{l} + \cos \frac{\Omega_c x}{l} \right) . \end{aligned} \quad (62)$$

Integration of eq. (36) now yields

$$\frac{\tilde{h}_\tau L_e}{EA} = -\frac{1}{2} \frac{8d}{l} \tilde{v}^s + \frac{8d}{l^2} \int_0^l \tilde{v} dx . \quad (63)$$

The substitution for \tilde{v} in eq. (63) from eq. (62) results in

$$\tilde{h}_\tau = \frac{EA}{L_e} \frac{\frac{1}{2} \epsilon (\kappa - 1)}{1 + \frac{\lambda^2}{\Omega_c^2} (\kappa - 1)} \tilde{v}^s . \quad (64)$$

With
$$H \frac{\partial \tilde{v}}{\partial x} \Big|_{x=0} = -\frac{1}{2} \epsilon \kappa \tilde{h}_\tau + \frac{1}{4} \frac{H}{l} \Omega_c^2 \kappa \tilde{v}^s \quad (65)$$

and
$$\tilde{h}^s = \left(1 + \frac{1}{4}\epsilon^2\kappa\right)\tilde{h}_\tau - \frac{1}{8}\frac{H}{l}\epsilon\Omega_c^2\kappa\tilde{v}^s \quad (66)$$

(according to eq. (28)) the stiffness function

$$k_{h,v}^s = \frac{EA}{L_e} \frac{\frac{1}{2}\epsilon \left[(\kappa - 1) - \frac{1}{4}\frac{\epsilon^2}{\lambda^2}\Omega_c^2\kappa \right]}{1 + \frac{\lambda^2}{\Omega_c^2}(\kappa - 1)} \quad (67)$$

is obtained. By again neglecting the term related to

$$\frac{\epsilon^2}{\lambda^2} = \frac{H}{EA} \frac{L_e}{l} \simeq \frac{H}{EA} \ll 1 \quad , \quad (68)$$

a simplified expression is obtained. It corresponds with the expression for $k_{\nu,u}^s$ given by eq. (52) (symmetry).

It is found from eq. (31) that

$$\tilde{v}^s = \frac{1}{2}\epsilon(\kappa - 1)\tilde{h}_\tau - \frac{1}{4}\frac{H}{l}\Omega_c^2\kappa\tilde{v}^s \quad , \quad (69)$$

from which the following stiffness function is obtained:

$$k_{\nu,v}^s = -\frac{EA}{L_e} \frac{\frac{1}{4}\frac{\epsilon^2}{\lambda^2}\Omega_c^2 \left[\kappa + \frac{\lambda^2}{\Omega_c^2}(\kappa - 1) \right]}{1 + \frac{\lambda^2}{\Omega_c^2}(\kappa - 1)} \quad . \quad (70)$$

When Ω_c is small, this expression is reduced to

$$k_{\nu,v}^s \Big|_{\Omega_c \simeq 0} = -\frac{1}{4} \frac{EA}{L_e} \frac{\epsilon^2}{\lambda^2} \Omega_c^2 = -\frac{1}{4} ml \omega_c^2 \quad . \quad (71)$$

This is a plausible result, as can be found directly, assuming that the cable moves like a rigid body.

The displacement is given by

$$\tilde{v} = \beta_v^s \cdot \tilde{v}^s \quad ,$$

where

$$\beta_v^s := \frac{1}{2} \frac{\tan \frac{\Omega_c}{2} \sin \frac{\Omega_c x}{l} + \cos \frac{\Omega_c x}{l} + \frac{\lambda^2}{\Omega_c^2} (\kappa - 1)}{1 + \frac{\lambda^2}{\Omega_c^2} (\kappa - 1)} = \frac{1}{2} \left(1 - \frac{\epsilon}{\lambda^2} \Omega_c^2 \beta_u^s \right) . \quad (72)$$

In the static case this correctly reduces to

$$\tilde{v}|_{\Omega_c \rightarrow 0} = \frac{1}{2} \tilde{v}^s . \quad (73)$$

Antisymmetric:



$$k_{h,v}^a := \frac{h^a}{v^a} = \frac{\tilde{h}^a}{\tilde{v}^a} \quad (74a)$$

$$k_{\nu,v}^a := \frac{\nu^a}{v^a} = \frac{\tilde{\nu}^a}{\tilde{v}^a} \quad (74b)$$

Figure 6. Vertical boundary displacement (antisymmetric)

Upon integration of eq. (36) with the displacement function $\tilde{v}(x)$, which is assumed to be antisymmetric, \tilde{h}_τ again is found to vanish. Nevertheless, the problem remains inhomogeneous here, because of the inhomogeneous boundary conditions. The solution is

$$\tilde{v} = \beta_v^a \cdot \tilde{v}^a \quad ,$$

where

$$\beta_v^a := \frac{1}{2} \left(\cot \frac{\Omega_c}{2} \sin \frac{\Omega_c x}{l} - \cos \frac{\Omega_c x}{l} \right) , \quad (75)$$

which in fact is an antisymmetric function. In the static case it becomes linear — as was to be expected.

Moreover, with

$$H \frac{\partial \tilde{v}}{\partial x} \Big|_{x=0} = \frac{H}{l} \frac{1}{\kappa} \tilde{v}^a \quad (76)$$

\tilde{h}^a is calculated from eq. (28) and from this it is found that

$$k_{h,v}^a = \frac{EA}{L_e} \frac{1}{2} \epsilon \frac{\epsilon^2}{\lambda^2} \frac{1}{\kappa} . \quad (77)$$

The static limiting value

$$k_{h,v}^a \Big|_{\Omega_c \rightarrow 0} = \frac{1}{2} \epsilon \frac{EA}{L_e} \frac{\epsilon^2}{\lambda^2} = \frac{1}{2} mg \quad (78)$$

in this case, however, is not identical with the correct value zero! This discrepancy (which is small in the total analysis) results from the basic assumption of a spatially constant τ , or rather h_τ , and the conclusion $h_\tau = 0$, which follows from eq. (36). A glance at eq. (28) shows that the force h_τ is indeed small but does not completely vanish (because $h^a|_{\Omega_c \rightarrow 0} = 0$). In view of this difficulty and in conformance with expression (58), which was derived for $k_{\nu,u}^a$ (symmetry), eq. (77) is replaced by

$$k_{h,v}^a = 0 . \quad (79)$$

The determination of ν^a , according to eq. (31), leads to

$$k_{\nu,v}^a = \frac{EA}{L_e} \frac{\epsilon^2}{\lambda^2} \frac{1}{\kappa} . \quad (80)$$

For the static case, the correct value

$$k_{\nu,v}^a \Big|_{\Omega_c \rightarrow 0} = \frac{EA}{L_e} \frac{\epsilon^2}{\lambda^2} = \frac{H}{l} \quad (81)$$

is obtained, which represents the rotational resistance of the cable. The difficulty which arose previously does not occur here, because h_τ affects ν^a to a lesser degree.

The displacement function β_v^a vanishes at midspan; at this point the displacement is

$$\tilde{v}_m = 0 . \quad (82)$$

4 Summary



Figure 7. Local force and displacement quantities

The elements k_{ij} ($i, j = 1, \dots, 4$) of the local dynamic stiffness matrix \mathbf{k} are defined by the transformation

$$\mathbf{f} = \mathbf{k} \cdot \boldsymbol{\delta} \quad , \quad (83)$$

in which

$$\mathbf{f} := \begin{pmatrix} f_1 \\ f_2 \\ f_3 \\ f_4 \end{pmatrix} ; \quad \boldsymbol{\delta} := \begin{pmatrix} \delta_1 \\ \delta_2 \\ \delta_3 \\ \delta_4 \end{pmatrix} \quad (84)$$

are the vectors of the local force and displacement quantities according to figure 7. Matrix \mathbf{k} is found by superposing the symmetric and antisymmetric contributions, which have been calculated in the previous two sections. The general formula required to perform the superposition is given by

$$\mathbf{k} = \mathbf{k}^s + \mathbf{k}^a \quad (85)$$

with the block matrices

$$\left. \begin{aligned} \mathbf{k}^s &:= \begin{pmatrix} \mathbf{k}_{h,u}^s & \mathbf{k}_{h,v}^s \\ \mathbf{k}_{\nu,u}^s & \mathbf{k}_{\nu,v}^s \end{pmatrix} \\ \mathbf{k}_{h,u}^s &:= k_{h,u}^s \begin{pmatrix} 1 & -1 \\ -1 & 1 \end{pmatrix} ; \quad \mathbf{k}_{h,v}^s := k_{h,v}^s \begin{pmatrix} -1 & -1 \\ 1 & 1 \end{pmatrix} \\ \mathbf{k}_{\nu,u}^s &:= k_{\nu,u}^s \begin{pmatrix} -1 & 1 \\ -1 & 1 \end{pmatrix} ; \quad \mathbf{k}_{\nu,v}^s := k_{\nu,v}^s \begin{pmatrix} 1 & 1 \\ 1 & 1 \end{pmatrix} \end{aligned} \right\} \quad (86)$$

and

$$\left. \begin{aligned}
\mathbf{k}^a &:= \begin{pmatrix} \mathbf{k}_{h,u}^a & \mathbf{k}_{h,v}^a \\ \mathbf{k}_{\nu,u}^a & \mathbf{k}_{\nu,v}^a \end{pmatrix} \\
\mathbf{k}_{h,u}^a &:= k_{h,u}^a \begin{pmatrix} 1 & 1 \\ 1 & 1 \end{pmatrix} \quad ; \quad \mathbf{k}_{h,v}^a := k_{h,v}^a \begin{pmatrix} -1 & 1 \\ -1 & 1 \end{pmatrix} \\
\mathbf{k}_{\nu,u}^a &:= k_{\nu,u}^a \begin{pmatrix} -1 & -1 \\ 1 & 1 \end{pmatrix} \quad ; \quad \mathbf{k}_{\nu,v}^a := k_{\nu,v}^a \begin{pmatrix} 1 & -1 \\ -1 & 1 \end{pmatrix}
\end{aligned} \right\} \quad (87)$$

Because $k_{h,u}^a = k_{h,v}^a = k_{\nu,u}^a = 0$, the more specific expression

$$\mathbf{k} = \begin{pmatrix} \mathbf{k}_{h,u}^s & \mathbf{k}_{h,v}^s \\ \mathbf{k}_{\nu,u}^s & (\mathbf{k}_{\nu,v}^s + \mathbf{k}_{\nu,v}^a) \end{pmatrix} \quad (88)$$

is obtained. Because $k_{h,v}^s = k_{\nu,u}^s$ and hence $\mathbf{k}_{h,v}^s = (\mathbf{k}_{\nu,u}^s)^\top$, this matrix is symmetric (but non-Hermitian if damping is taken into account).

The vertical displacement is exclusively determined by the boundary displacements u^s , v^s and v^a (because $\beta_u^a \equiv 0$). The total displacement is given by

$$v = -\beta_u^s(\delta_1 - \delta_2) + \beta_v^s(\delta_3 + \delta_4) - \beta_v^a(\delta_3 - \delta_4) \quad (89)$$

It should be noted that the stiffness and displacement terms appearing in eqs. (88) and (89) become infinite for certain values of Ω_c . In the case of real Ω_c , these values must coincide with the natural frequencies of an undamped cable which is suspended from rigid end supports. This condition leads to frequency equations which conform to the findings of study [2].

4 Generalization to the Inclined Cable

Extending the theory of the horizontal cable developed in [2], Irvine [4] gave solutions for the free vibration of an inclined, rigidly supported cable. It can be shown that only one additional assumption is necessary for this extension: that the weight component parallel to the cable chord can be neglected.

The results of [4] correspond well with those of the more precise theory of Triantafyllou [5] and [6], as long as the cable parameters λ^2 and ϵ as well as the angle of inclination Θ , do not exceed certain limits. In particular, λ^2 should maintain a certain distance (about 20 %) from the so-called 'cross-over' points $4n^2\pi^2$ ($n = 1, 2, \dots$), ϵ and Θ should not be too large.

The theory presented here corresponds to study [2] in its essential assumptions. Neg-

lecting once again the weight component parallel to the cable chord, the transition to an inclined cable is made by the following substitutions:

- g is replaced by the gravitational component $g \cos \Theta$, which acts perpendicular to the cable chord (where Θ is the chord inclination),
- the quantity $T_\Theta = H / \cos \Theta$ must be substituted for the horizontal component H of the static cable tension; it represents the static cable tension at the section where the cable is parallel to the chord, and corresponds approximately to the average cable tension.

The other free parameters remain unchanged, but now l denotes the chord length and d is the sag perpendicular to the chord. All coordinates and displacements relate to the local coordinate system, where the x -axis is parallel to the chord.

The dependent parameters become

$$\Omega = \omega l \sqrt{\frac{m}{T_\Theta}} ; \quad \Omega_c = \omega_c l \sqrt{\frac{m}{T_\Theta}} \quad (90)$$

$$\lambda^2 = \left(\frac{mgl}{T_\Theta} \right)^2 \frac{EA l}{T_\Theta L_e} \cos^2 \Theta \quad (91)$$

$$\epsilon = \frac{mgl}{T_\Theta} \cos \Theta = \frac{8d}{l} , \quad (92)$$

where

$$T_\Theta = H / \cos \Theta \quad (93)$$

$$L_e \simeq l \left[1 + 8 \left(\frac{d}{l} \right)^2 \right] . \quad (94)$$

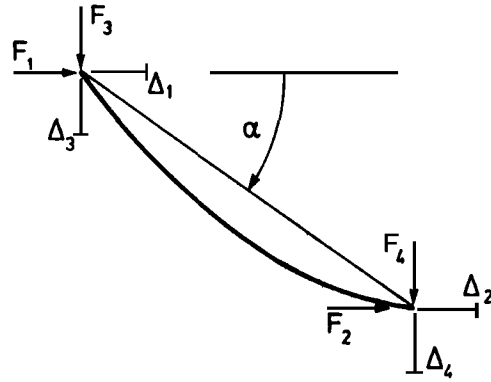
With these new terms, the theory developed here can be used for an inclined cable, if the limiting conditions

$$\left. \begin{array}{l} \lambda^2 \leq 24 \\ \text{and} \\ \Theta \leq 60^\circ \quad \text{and} \quad \epsilon \leq 0.10 \quad (d/l \leq 1/80) \\ \text{or} \quad \Theta \leq 30^\circ \quad \text{and} \quad \epsilon \leq 0.24 \quad (d/l \leq 1/33) \end{array} \right\} \quad (95a)$$

are satisfied. The specified range of validity is inferred from the numeric results of studies [4] and [6]; a conservative criterion relative to λ^2 is employed, hereby taking into account that the problems investigated are similar but not identical (movable supports in this paper, fixed supports in [4] and [6]). Condition (8) must be replaced by

$$\sqrt{\frac{EA}{T\Theta}} \gg 1 . \quad (95b)$$

5 Transformation to Global Coordinates



The global force and displacement vectors (according to fig. 8)

Figure 8. Global force and displacement quantities

$$\mathbf{F} := \begin{pmatrix} F_1 \\ F_2 \\ F_3 \\ F_4 \end{pmatrix} ; \quad \mathbf{\Delta} := \begin{pmatrix} \Delta_1 \\ \Delta_2 \\ \Delta_3 \\ \Delta_4 \end{pmatrix} \quad (96)$$

are converted into the local quantities given by figure 7 through the orthogonal transformations

$$\left. \begin{aligned} \mathbf{f} &= \mathbf{T} \cdot \mathbf{F} ; \quad \boldsymbol{\delta} = \mathbf{T} \cdot \mathbf{\Delta} \\ \mathbf{T} &:= \begin{pmatrix} E \cos \alpha & E \sin \alpha \\ -E \sin \alpha & E \cos \alpha \end{pmatrix} ; \quad \mathbf{E} := \begin{pmatrix} 1 & 0 \\ 0 & 1 \end{pmatrix} . \end{aligned} \right\} \quad (97)$$

(In practical applications, the angle of rotation α is often equal to the inclination angle Θ , defined in the previous section.) When substituting for the local vectors into eq. (83) and premultiplying by \mathbf{T}^{-1} , this leads to

$$\mathbf{F} = \mathbf{K} \cdot \Delta , \quad (98)$$

where

$$\mathbf{K} := \mathbf{T}^{-1} \mathbf{k} \mathbf{T} = \mathbf{T}^\top \mathbf{k} \mathbf{T} \quad (99)$$

is the global dynamic stiffness matrix. The application of the operation instruction (99) to the local matrix \mathbf{k} given by eq. (88), yields the symmetric block matrix

$$\mathbf{K} = \begin{pmatrix} K_{aa} & K_{ab} \\ K_{ba} & K_{bb} \end{pmatrix} ,$$

where

$$\left. \begin{aligned} K_{aa} &:= \mathbf{k}_{h,u}^s \cos^2 \alpha - (\mathbf{k}_{h,v}^s + \mathbf{k}_{\nu,u}^s) \cos \alpha \sin \alpha + (\mathbf{k}_{\nu,v}^s + \mathbf{k}_{\nu,v}^a) \sin^2 \alpha \\ K_{ab} &:= \mathbf{k}_{h,u}^s \cos \alpha \sin \alpha + \mathbf{k}_{h,v}^s \cos^2 \alpha - \mathbf{k}_{\nu,u}^s \sin^2 \alpha \\ &\quad - (\mathbf{k}_{\nu,v}^s + \mathbf{k}_{\nu,v}^a) \cos \alpha \sin \alpha \\ K_{ba} &:= \mathbf{k}_{h,u}^s \cos \alpha \sin \alpha - \mathbf{k}_{h,v}^s \sin^2 \alpha + \mathbf{k}_{\nu,u}^s \cos^2 \alpha \\ &\quad - (\mathbf{k}_{\nu,v}^s + \mathbf{k}_{\nu,v}^a) \cos \alpha \sin \alpha \\ K_{bb} &:= \mathbf{k}_{h,u}^s \sin^2 \alpha + (\mathbf{k}_{h,v}^s + \mathbf{k}_{\nu,u}^s) \cos \alpha \sin \alpha + (\mathbf{k}_{\nu,v}^s + \mathbf{k}_{\nu,v}^a) \cos^2 \alpha . \end{aligned} \right\} \quad (100)$$

The submatrices which appear in these expressions are given by eqs. (86) and (87).

In systems such as guyed masts and cable-stayed bridges, the axial deformations of the beams are relatively small. If the axes of the global coordinate system lie parallel to the beams, the elements K_{11} , K_{44} , and probably also K_{14} , K_{41} of the dynamic stiffness matrix \mathbf{K} will be of special interest. By following eq. (100) and utilizing the properties of symmetry previously stated, it is found that

$$\left. \begin{aligned} K_{11} &= \mathbf{k}_{h,u}^s \cos^2 \alpha + 2\mathbf{k}_{\nu,u}^s \cos \alpha \sin \alpha + (\mathbf{k}_{\nu,v}^s + \mathbf{k}_{\nu,v}^a) \sin^2 \alpha \\ K_{14} &= K_{41} = - \left[\mathbf{k}_{h,u}^s + (\mathbf{k}_{\nu,v}^s - \mathbf{k}_{\nu,v}^a) \right] \cos \alpha \sin \alpha - \mathbf{k}_{\nu,u}^s \\ K_{44} &= \mathbf{k}_{h,u}^s \sin^2 \alpha + 2\mathbf{k}_{\nu,u}^s \cos \alpha \sin \alpha + (\mathbf{k}_{\nu,v}^s + \mathbf{k}_{\nu,v}^a) \cos^2 \alpha . \end{aligned} \right\} \quad (101)$$

By neglecting several components of frequently minor influence, these equations are reduced to the simplified expressions

$$\left. \begin{aligned}
K_{11} &= k_{h,u}^s \cos^2 \alpha + 2k_{\nu,u}^s \cos \alpha \sin \alpha \\
K_{14} &= K_{41} = -k_{h,u}^s \cos \alpha \sin \alpha - k_{\nu,u}^s \\
K_{44} &= k_{h,u}^s \sin^2 \alpha + 2k_{\nu,u}^s \cos \alpha \sin \alpha ,
\end{aligned} \right\} \quad (102)$$

which will often give sufficiently accurate results.

The total displacement perpendicular to the cable chord as a function of the global boundary displacements ensues from eqs. (89) and (97). The following expression is obtained:

$$\begin{aligned}
v &= -\beta_u^s [(\Delta_1 - \Delta_2) \cos \alpha + (\Delta_3 - \Delta_4) \sin \alpha] \\
&\quad -\beta_v^s [(\Delta_1 + \Delta_2) \sin \alpha - (\Delta_3 + \Delta_4) \cos \alpha] \\
&\quad +\beta_v^a [(\Delta_1 - \Delta_2) \sin \alpha - (\Delta_3 - \Delta_4) \cos \alpha] .
\end{aligned} \quad (103)$$

It should be remembered that the given equations are valid for displacements and forces according to approach (32) only.

Extension of the given theory to the spatial problem is possible without major difficulty. In linearized theory the in-plane motion is uncoupled from the transverse horizontal motion (cf.[2]). The spatial dynamic cable stiffness can therefore be described by a block diagonal matrix, if an appropriate coordinate system is chosen. Its first diagonal-block is already given by the 4*4 matrix of eq. (100); the second one, a 2*2 matrix, must still be derived.

The action of fluid forces must be considered, if the investigated cable is immersed in weighty mediums like water. This can be accomplished by adequately establishing the parameters m , g and ξ (cf.[7]). For a cable in air, this only concerns the damping parameter ξ .

8 Example Analysis and Discussion

The numeric application of the derived formulas requires complex arithmetic. When complex numbers are written in the general form

$$z = z' + iz'' ; \quad z', z'' \in \mathcal{R} , \quad (104)$$

then trigonometrical functions are given by (cf.[10]):

$$\left. \begin{aligned} \sin z &= \sin z' \cosh z'' + i \cos z' \sinh z'' \\ \cos z &= \cos z' \cosh z'' - i \sin z' \sinh z'' \\ \tan z &= \frac{\sin 2z' + i \sinh 2z''}{\cos 2z' + \cosh 2z''} = \frac{1}{\cot z} . \end{aligned} \right\} \quad (105)$$

Example 1:

The dynamic stiffness K_{11} and the displacement at midspan $v_m(\Delta_1)$ are calculated for the parameters

$$\frac{mgl}{T_\Theta} = 0.217 , \quad \frac{T_\Theta}{EA} = 0.000633 , \quad \alpha = \Theta = 55.86^\circ , \quad \xi = \frac{0.14}{\Omega/\pi} ,$$

as functions of real Ω .

From eqs. (94), (91) and (92) follows

$$L_e/l = 1.002 \simeq 1 , \quad \lambda^2 = 23.48 , \quad \epsilon = 0.1218 ;$$

the limits of validity established by eqs. (95a) are nearly met. Condition (95b) is likewise satisfied.

The stiffness function K_{11} was computed according to eq. (101) and — for purposes of comparison — according to the simplified eq. (102). The contribution $k_{h,u}^s$ was calculated by alternatively applying eq. (48) and the less precise eq. (49). In the range of extreme values, the K_{11} , determined from various equations, deviate at most 3% in their real and imaginary parts.

In order to obtain dimensionless graphs, the dynamic stiffness K_{11} is related to the elastic part $K_{11}^{t,e}$ of the static stiffness K_{11}^t of a taut wire (i.e. a straight rod)

$$K_{11}^t = K_{11}^{t,e} \left(1 + \frac{T_\Theta}{EA} \tan^2 \alpha \right) ; \quad K_{11}^{t,e} := \frac{EA}{l} \cos^2 \alpha . \quad (106)$$

Utilizing the simplified eqs. (49) and (102), and neglecting the factor l/L_e , the expression

$$K_{11}^* := \frac{K_{11}}{K_{11}^{t,e}} = \frac{1 + \epsilon \tan \alpha (\kappa - 1)}{1 + \frac{\lambda^2}{\Omega_c^2} (\kappa - 1)} \quad (107)$$

is obtained, which provides a reasonably accurate approximation for the cable considered here. The real and imaginary parts of this function are depicted in figure 9.

A comparison of these curves with the curves that Davenport & Steels [7] calculated for the same parameters shows similarity, but not total agreement. Their solution requires numerical evaluation of infinite series and so cannot be directly compared to the closed-form solution given here. It appears, however, that the contribution of $k_{\nu,u}^s$ was omitted. This term is equal to $k_{h,v}^s$ (which they considered) and, according to eq. (100), has the same influence on the total stiffness. When expression (107) is truncated by this contribution (by dividing the second term in the numerator by 2), the curves plotted in paper [7] can be precisely reproduced. Moreover, it then coincides with a closed-form expression given in [7] for the special case of an undamped cable. In this example, $k_{\nu,u}^s$ contributes approximately 15% to the total stiffness and therefore should not be neglected.

The displacement expression (103), with only Δ_1 being non-zero, reduces to

$$v = v(\Delta_1) = -[\beta_u^s \cos \alpha + (\beta_v^s - \beta_v^a) \sin \alpha] \Delta_1 \quad (108)$$

At midspan, β_v^a vanishes. When eqs. (53) and (72) are substituted for the remaining displacement functions, it is found that

$$\frac{v_m}{\Delta_1} = \frac{\tilde{v}_m}{\tilde{\Delta}_1} = -\frac{\frac{1}{\epsilon} \frac{\lambda^2}{\Omega_c^2} \cos \alpha \left[1 - \frac{1}{\cos(\Omega_c/2)} \right] + \frac{1}{2} \sin \alpha \left[\frac{1}{\cos(\Omega_c/2)} + \frac{\lambda^2}{\Omega_c^2} (\kappa - 1) \right]}{1 + \frac{\lambda^2}{\Omega_c^2} (\kappa - 1)} \quad (109)$$

The dimensionless displacement computed according to this expression is depicted in the lower part of figure 9. As expected, its real and imaginary parts correspond with those of the dynamic stiffness. The influence of β_v^s on the total displacement amounts to about 15% in this analysis.

For the special case of an undamped cable, Irvine [3] gave closed-form expressions for the dynamic stiffness K_{11} and the displacement $v(\Delta_1)$. When the simplified expression (107) and the term (108) are adapted to apply to an undamped cable, and the contributions of $k_{h,v}^s$, $k_{\nu,u}^s$ and β_v^s , β_v^a are omitted, these expressions coincide with Irvine's equations; depending on the respective values of these contributions, the equations given in [3] are less accurate.

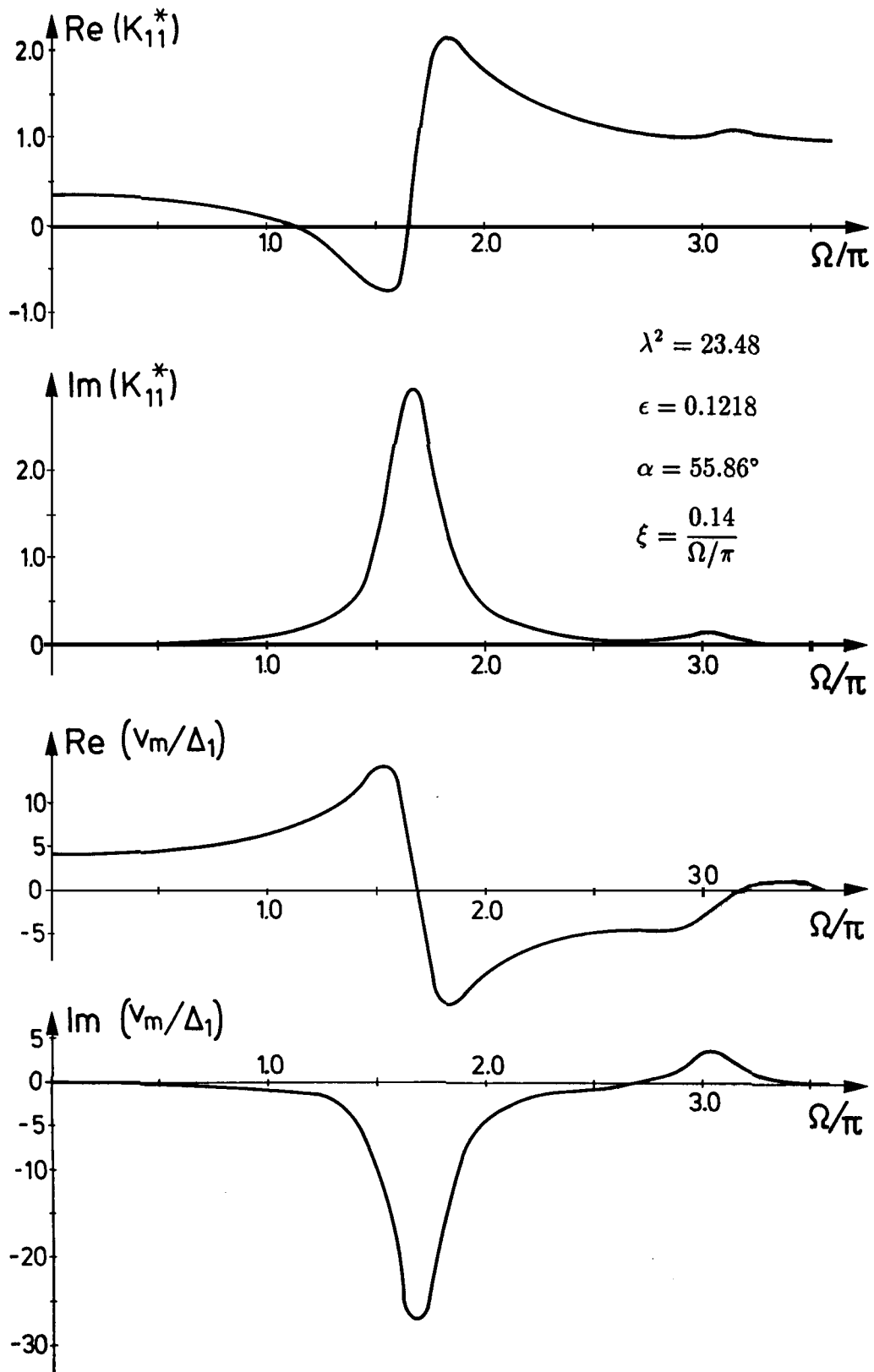


Figure 9. Dynamic stiffness function and displacement at midspan (example 1)

Example 2:

The dynamic stiffness K_{44} and the displacement at midspan $v_m(\Delta_4)$ are calculated for the parameters

$$l = 200 \text{ m} , \quad \frac{mg}{A} = 0.08 \text{ MN/m}^3 , \quad \frac{T_\Theta}{A} = 500 \text{ MPa}$$

$$E = 200\,000 \text{ MPa} , \quad \alpha = \Theta = 30^\circ , \quad \xi = 0.01 ,$$

as functions of real Ω .

From eqs. (94), (91) and (92)

$$L_e/l = 1.0001 \simeq 1 , \quad \lambda^2 = 0.3072 , \quad \epsilon = 0.02771$$

is obtained. The limits of validity defined by eq. (95a) are safely met and condition (95b) is satisfied.

The influence of various simplifications in the analysis of K_{44} is also investigated here, as in example 1. In this case, however, the use of the simplified eq. (102) — that is, the neglect of $k_{\nu,\nu}^s$ and $k_{\nu,\nu}^a$ — leads to completely wrong results! It is of particular interest that the imaginary part K_{44}'' of the total stiffness becomes negative due to the omission of $k_{\nu,\nu}^s$. The work performed by the boundary force F_4 within one period is given by

$$W = \int_0^{2\pi/\omega} (K_{44} \Delta_4)' \left(\frac{\partial \Delta_4}{\partial t} \right)' dt = \pi K_{44}'' |\Delta_4|^2 . \quad (110)$$

Because this work is positive (as long as it is ξ), negative K_{44}'' may not occur; otherwise, this system would be a *perpetuum mobile*! The contribution of $k_{\nu,\nu}^a$ must be considered too, because considerable variations occur within the range of the natural frequencies associated with antisymmetric modes (i.e. of a cable fixed at both ends). Furthermore, comparative analysis shows that the contribution $k_{h,u}^s$ can be calculated again by the simplified eq. (49) without a major loss of accuracy.

These results seem to be typical for tightly stretched inclined cables as they are employed in cable-stayed bridges.

The dynamic stiffness is again related to the elastic part $K_{44}^{t,e}$ of the static stiffness K_{44}^t of a taut wire

$$K_{44}^t = K_{44}^{t,e} \left(1 + \frac{T_\Theta}{EA} \cot^2 \alpha \right) ; \quad K_{44}^{t,e} := \frac{EA}{l} \sin^2 \alpha . \quad (111)$$

From the complete eq. (101) and the simplified eq. (49) it is found that

$$K_{44}^* := \frac{K_{44}}{K_{44}^{t,e}} = \frac{1 + \epsilon \cot \alpha (\kappa - 1) - \frac{1}{4} \varrho \Omega_c^2 \left[\kappa + \frac{\lambda^2}{\Omega_c^2} (\kappa - 1) \right]}{1 + \frac{\lambda^2}{\Omega_c^2} (\kappa - 1)} + \frac{\varrho}{\kappa}, \quad (112)$$

where the abbreviation

$$\varrho := \frac{\epsilon^2}{\lambda^2} \cot^2 \alpha \simeq \frac{T_\Theta}{EA} \cot^2 \alpha \quad (113)$$

is used. The factor l/L_e is insignificant and is again neglected. The curves resulting from equation (112) are shown in figure 10.

The variations in the range of the natural frequency associated with the first symmetric mode are small. The numeric analysis showed that here the various stiffness contributions nearly cancel each other. The variations in the vicinity of the first antisymmetric and second symmetric natural frequencies predominate!

Compared to example 1, the ‘resonance tubes’ of the stiffness functions are much narrower here; the variations are smaller and K'_{44} remains positive. As a review of the applied equations shows, these differences are due to ϵ and λ^2 becoming much smaller. Consequently, the sag as well as the influence of the geometrical stiffness (which is mainly induced by transverse cable displacements) decrease. The elastic stiffness, now being relatively small and therefore of dominant influence, is quasi-static! Hence, the resulting stiffness function approximates in a wide range (and especially for small Ω) the constant value which would have been determined for a massless taut wire. Appreciable transverse displacements and the implied dynamic stiffness effects occur only in the direct proximity of resonance frequencies. Therefore, in the case of tightly stretched cables, less damping seems to be necessary in order to limit the variations of the dynamic stiffness functions.

The greater prominence of higher natural frequencies has its numeric origin in a larger ϱ . In addition to ϵ and λ^2 , this parameter is likewise of importance. It corresponds to the ratio of rotational to elastic stiffness of a taut wire (see equations (111) and (113)).

Under the same conditions, Veletsos & Darbre [8] have derived a formula for the dynamic stiffness K_{11} . It can be compared with expression (112), provided $\cot \alpha$ is first replaced by $\tan \alpha$, in order to accomplish a transition from K_{44}^* to K_{11}^* . Initially, exact agreement could not be established. A detailed review of paper [8], however, showed that an error apparently occurred at the derivation of its central equation (38).

When carrying out this derivation as specified, an expression which differs from that given in [8] is obtained. This result is also somewhat simpler: the denominator $[1 - i(2\pi\zeta/\Phi)]$ within the first part of [8, eq. (38)] must be replaced by unity. The equation modified in this way can be exactly transformed into expression (112) (except for the factor l/L_e which is here neglected).

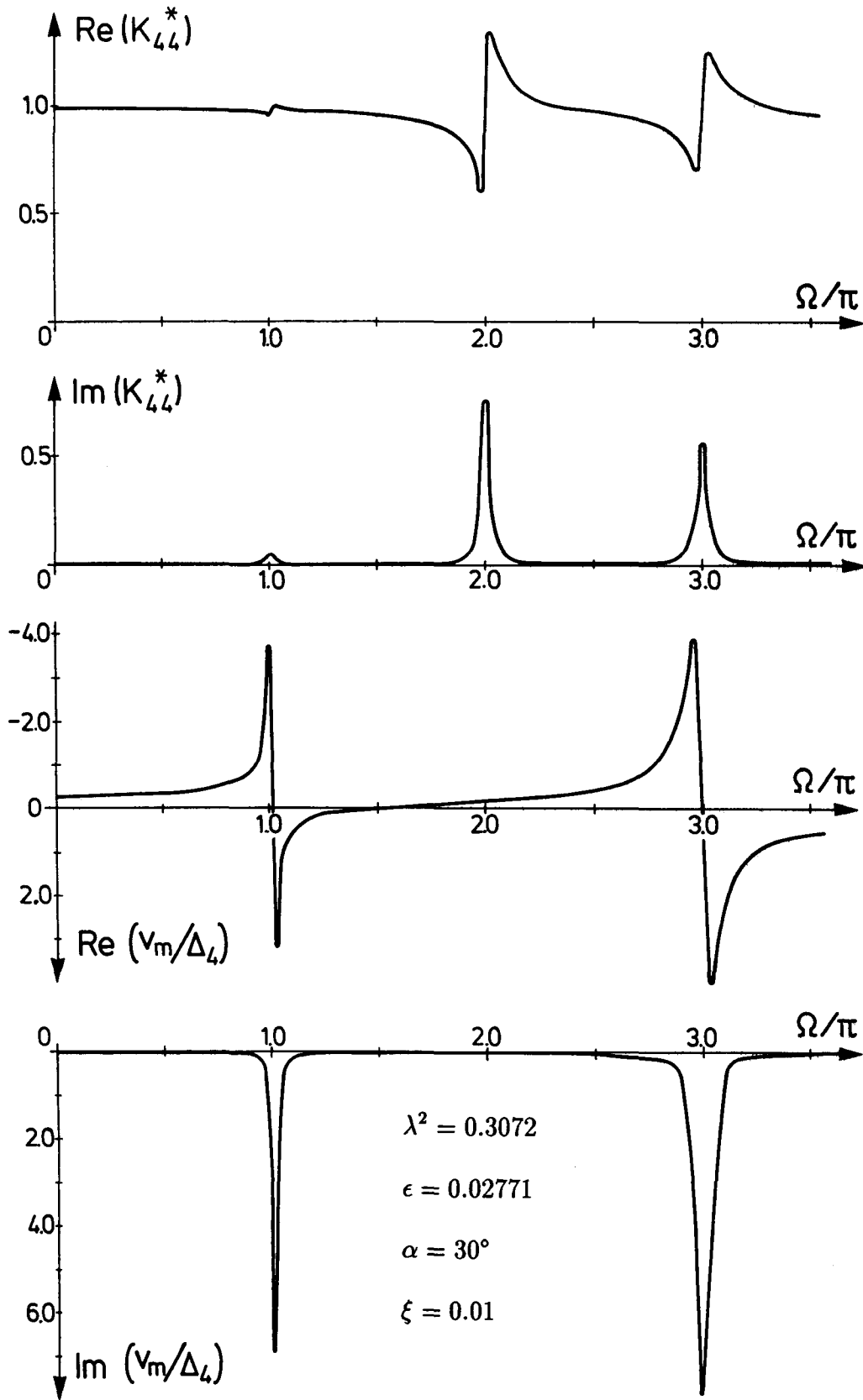


Figure 10. Dynamic stiffness function and displacement at midspan (example 2)

Both expressions remain slightly different in their external form, for they were obtained in different ways: the separation into symmetric and antisymmetric contributions is less distinct in [8] than in the formula given in this paper. Without separation, eq. (112) can be converted into the somewhat shorter expression

$$K_{44}^* = \frac{[1 + \frac{1}{2}\epsilon \cot \alpha (\kappa - 1)]^2}{1 + \frac{\lambda^2}{\Omega_c^2}(\kappa - 1)} + \rho \Omega_c \cot \Omega_c , \quad (112a)$$

which corresponds in its formal arrangement with eqs. (38) and (41) of [8].

A comparison of the derivations and results presented in this study with those given in paper [8] shows the advantage of the limitation to trigonometrical solution functions with complex arguments. Algebraic effort is reduced to a minimum. The resulting equations are more concise and take the same external shape for damped and undamped cables (for an undamped cable, Ω_c is simply replaced by Ω).

The simplified solution (39) given in [8] is the closed-form counterpart of Davenport's [7] series solution. According to the findings presented above (example 1), the second term of the numerator of [8, eq. (39)] should be multiplied by factor 2. The expression then corresponds with eq. (107) of this paper. As can be seen in eq. (112), accuracy of the simplified solution decreases with growing ρ .

The displacement expression eq. (103) reduces to

$$v = v(\Delta_4) = [\beta_u^s \sin \alpha + (\beta_v^s + \beta_v^a) \cos \alpha] \Delta_4 . \quad (114)$$

From this follows a formula for the displacement at midspan, which is similar to eq. (109). Its numeric evaluation is reproduced in figure 10.

In the range of the first symmetric natural frequencies, a strong vibration excitement occurs in spite of the nearly undisturbed course of the stiffness functions. The resonance excitement which corresponds to the first antisymmetric natural frequency does not appear, because only the displacement amplitude at midspan is regarded.

An experimental verification of the theory presented here would be valuable, especially for a more accurate delimitation of the range of validity. In view of the partial similarity of the theoretical results, the tests of Davenport & Steels [7] are cited for principle verification. Their comparison of analytical results with dynamic tests of a model cable immersed in a liquid bath produced partially excellent agreement. The previously established and analytically considered parameters (especially the damping coefficient), however, had to be greatly altered in order to obtain a closer fit to the experimental data. This difficulty seems to diminish when using the equations given in this study.

The experimental results [7] also indicate a resonance effect in the range of the antisymmetric natural frequency $\Omega = 2\pi$. This is predicted by the complete solutions (101) and the resulting equation (112), given here.

Notation

A	effective cross-sectional area of cable
c	damping force per unit length and velocity
d	cable sag perpendicular to cable chord
ds	length of differential cable element
E	Young's modulus of elasticity
F_i	global boundary force according to figure 8
\mathbf{F}	vector of global boundary forces
f_i	local boundary force according to figure 7
\mathbf{f}	vector of local boundary forces
g	gravitational acceleration (decreased by buoyancy effect)
H	horizontal component of static cable tension
h	dynamic part of the horizontal component of total cable tension
h_r	force quantity according to eq. (20)
K_{ij}	element of the global dynamic stiffness matrix
K_{ij}^*	dimensionless dynamic stiffness function defined by eqs. (107), (112)
\mathbf{K}_{mn}	submatrices according to eqs. (100)
\mathbf{K}	global dynamic stiffness matrix defined by eq. (98)
k_{ij}	element of the local dynamic stiffness matrix
$k_{p,q}^r$	dynamic stiffness function related to a specified set of boundary displacements
$\mathbf{k}_{p,q}^r$	submatrices according to eqs. (86), (87)
\mathbf{k}	local dynamic stiffness matrix defined by eq. (83)
L_e	cable parameter according to eq. (40), resp. eq. (94)
l	length of cable chord
m	cable mass per unit length (increased by virtual mass effect due to fluid)
T	static cable tension

T_{Θ}	static cable tension at section where cable is parallel to chord, cf. eq. (93)
T	transformation matrix according to eqs. (97)
t	time
u	displacement parallel to cable chord
V	vertical component of static cable tension
v	displacement perpendicular to cable chord
x	coordinate of static cable line parallel to cable chord
y	coordinate of static cable line perpendicular to cable chord
α	angle of rotation of the transformation to global coordinates, figure 8
β_q^r	dimensionless cable displacement produced by a specified set of boundary displacements
Δ_i	global boundary displacement according to figure 8
Δ	vector of global boundary displacements
δ_i	local boundary displacement according to figure 7
δ	vector of local boundary displacements
ε	dynamic part of axial cable strain
ϵ	cable parameter according to eq. (47), resp. eq. (92)
Θ	angle of inclination of cable chord (measured from a horizontal line)
κ	Ω_c -dependent auxiliary term, eq. (43)
λ^2	cable parameter according to eq. (42), resp. eq. (91)
ν	dynamic part of the vertical component of total cable tension
ξ	dimensionless damping parameter, eqs. (34)
ϱ	cable parameter according to eq. (113)
τ	dynamic part of total cable tension
Ω	dimensionless frequency, eqs. (35), resp. eqs. (90)
Ω_c	dimensionless frequency-damping parameter, eqs. (35), resp. eqs. (90)
ω	circular frequency of a motion according to eqs. (32)
ω_c	frequency-damping parameter defined by eqs. (34)

References

- [1] R. W. Clough, J. Penzien: Dynamics of Structures. McGraw-Hill, New York (1975)
- [2] H. M. Irvine, T. K. Caughey: The Linear Theory of Free Vibrations of a Suspended Cable. Proceedings of the Royal Society of London, Series A, Vol. 341, pp. 299–315 (1974)
- [3] H. M. Irvine: Cable Structures. MIT Press, Cambridge, Massachusetts (1981)
- [4] H. M. Irvine: Free Vibrations of Inclined Cables. ASCE, Journal of the Structural Division, Vol. 104, No. ST 2, pp. 343–347 (1978)
- [5] M. S. Triantafyllou: The Dynamics of Taut Inclined Cables. Quarterly Journal of Mechanics and Applied Mathematics, Vol. 37, Pt. 3, pp. 421–440 (1984)
- [6] M. S. Triantafyllou, L. Grinfogel: Natural Frequencies and Modes of Inclined Cables. ASCE, Journal of Structural Engineering, Vol. 112, No. 1, pp. 139–148 (1986)
- [7] A. G. Davenport, G. N. Steels: Dynamic Behavior of Massive Guy Cables. ASCE, Journ. Struct. Div., Vol. 91, No. ST 2, pp. 43–70 (1965)
- [8] A. S. Veletsos, G. R. Darbre: Dynamic Stiffness of Parabolic Cables. Earthquake Engineering and Structural Dynamics, Vol. 11, No. 3, pp. 367–401 (1983)
- [9] U. Starossek: Die Dynamik des durchhängenden Seiles. Institut für Tragwerksentwurf und -konstruktion, Universität Stuttgart (1989)
- [10] I. N. Bronstein, K. A. Semendjajew: Taschenbuch der Mathematik. Verlag Harri Deutsch, Thun (1985)